Issues in validation of performances of piezoelectric vibration-based energy harvesters

Saša Zelenika [a], David Blažević [*a]

[a] University of Rijeka, Centre for Micro and Nano Sciences and Technologies & Faculty of Engineering, Vukovarska 58, 51000 Rijeka, CROATIA

ABSTRACT

Vibration energy harvesting devices based on piezoelectric bimorphs have attracted widespread attention. In this work experimental set-ups are developed to assess the performances of commercially available piezoelectric energy harvesters. Bending tests allow determining the equivalent bending stiffness of the scavengers. On the other hand, dynamic tests allow obtaining frequency response functions in terms of produced voltage and power outputs vs. base acceleration around the fundamental resonance frequency. The results allow determining the influence of the voltage feedback on the dynamic response of the devices, the dependence of output voltages and powers on the applied resistive loads, the values of the loads and frequencies for which the output power is maximized, as well as the comparison of the experimental data with those obtained by using the recently developed coupled electromechanical modal model. All of this creates the preconditions for the development of optimized vibration energy harvesting devices.

Keywords: vibration energy harvesting, piezoelectric material, electromechanical coupling analysis, experimental assessment

1. INTRODUCTION

Harvesting of environmental energy, i.e. the process of collecting low level ambient energy and its conversion into electric power via devices based on photovoltaics, thermoelectric principles, RF and radiation sources, electromagnetic conversion or scavenging of kinetic energy (e.g. fluid flow or vibrations) has attracted widespread research and industrial attention. This tendency is especially evident in the development of wireless sensor networks, but also in healthcare and body sensors, structural health monitoring, smart packaging solutions, transportation, communication systems, unmanned air vehicles and aerospace, structural biology, robotics, MEMS devices, everyday's' gadgets and toys and many other sectors and potential applications.[1-9]

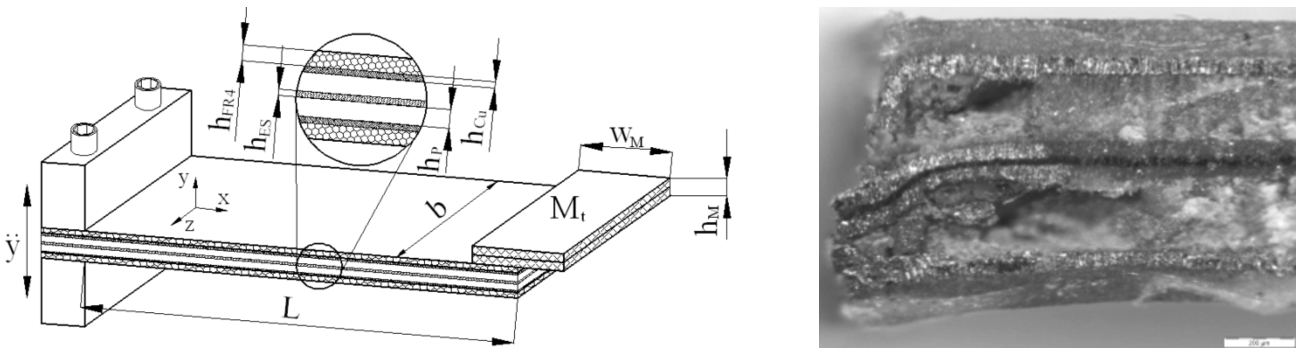

(a) (b)

Figure 1. Scheme of the structure of a commercial MIDE vibration energy harvesting device with its main dimensional parameters (a) and cross-section of the device seen through a stereomicroscope (b).

[*] dablazev@riteh.hr; phone + 385 – (0)51 - 651585; fax +385 – (0)51 - 651416; www.riteh.uniri.hr & www.cmnzt.uniri.hr

Harvesting of vibration energy can be performed via piezoelectric, electromagnetic and electrostatic devices.[10] The usage of piezoelectric materials is particularly advantageous due to design simplicity, miniaturization and integration potential, high energy density, as well as the inherent linearity of the mechanical behavior and of the electromechanical coupling. Vibration-based energy harvesting via cantilevers covered with piezoelectric material that are excited at the fixation with harmonic vibrations, has received the greatest attention.[1, 10-18] In fact, several vibration energy harvesters are already commercially available.[8-9, 19-24] Although ideally the used design configuration is that of a "bimorph" cantilever having two layers of piezoelectric material bonded onto a metallic substrate, the actual design of commercially available solutions can be quite different. The herein considered MIDE vibration energy harvesters[23] have, in fact, a very intricate structure (Fig. 1a) composed of multiple layers of: woven fiberglass reinforced epoxy laminate sheets (FR4), epoxy adhesive films, copper electrodes, layers of piezoelectric materials and copper clad polyimide laminates (ESPANEX). This structure was examined optically by using an Olympus type SZX16 stereomicroscope (Fig. 1b),[25] as well as via an analysis performed on an Oxford instruments INCA-based energy dispersive X-ray spectroscopy apparatus where electrons emitted by a scanning electron microscope (SEM) hit the analyzed sample inducing a resulting emission of X-rays.[26] Nevertheless, the intricate structure makes the retrieval of all the needed electromechanical data and the modeling of the behavior of the whole device very complex.

In this work the characterization of the dynamic performances of the considered devices is performed with the aim of determining the respective frequency response functions (FRFs) and thus establishing the influence of the system characteristic parameters (i.e. excitation parameters and downstream electrical loads) on the obtained responses (voltage and power outputs as well as their maximal values). Suitable experimental set-ups for the determination of the equivalent bending stiffness and the FRFs are thus developed and described. It becomes therefore possible to correlate the behavior of the off-the-shelf piezoelectric harvesters to the recently developed coupled electromechanical modal model.[14] This will make possible, in the following phase of the work, the development of custom vibration energy harvesting devices with optimized performances.

2. UNCOUPLED DYNAMIC MODEL

2.1 Uncoupled modal model

In order to have a quick yet accurate tool for the determination of the response of a piezoelectric vibration-based harvester and the tuning of its response to the excitation source, in a first instance a modal model of the mere mechanical (i.e. uncoupled) behavior of a cantilever beam loaded at the free end with a proof mass M_t is considered (Fig. 2).

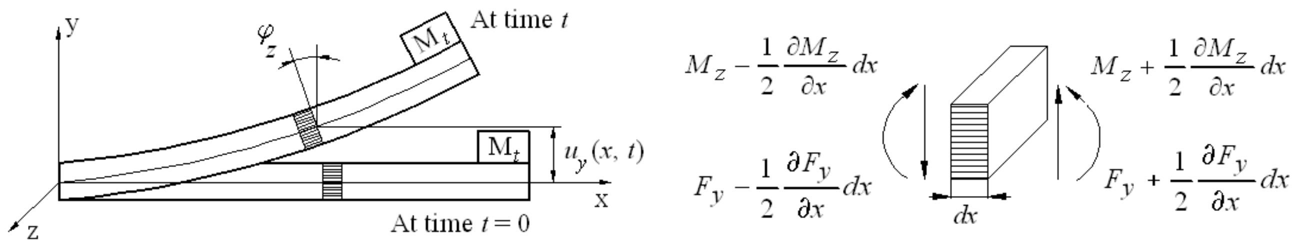

Figure 2. Model of the cantilever with a tip mass.

Indicating with E the Young's modulus of the material the cantilever is made of, with ρ its density, with I_z the second moment of inertia of the cross section of area A and with $u_y(x, t)$ beam's deflection in y direction relative to the fixture, the force and moment equilibrium of the classical Euler-Bernoulli beam (i.e. supposing that the sections of the cantilever remain plane, while shear deformation and cross-section rotary inertia are negligible) is thus considered. The bending stiffness $k(x)=E(x)\cdot I_z(x)$ and the mass distribution along the cantilever length $m(x)=\rho(x)\cdot A(x)$ are regarded as constants:[27]

$$m\frac{d^2u_y}{dt^2} = -\frac{\partial^2}{\partial x^2}\left[k\frac{\partial^2 u_y}{\partial x^2}\right] \tag{1}$$

Following the standard modal expansion method, the variables are separated in time and space domains so that, for n uncoupled vibration modes, the deflection of the cantilever beam can be expressed as a linear combination of eigenfunctions:

$$u_y(x,t) = \sum_{n=1}^{\infty} \phi_n(x) \cdot \eta_n(t) \tag{2}$$

where, for each n-th mode of vibrations, $\phi_n(x)$ is the respective eigenfunction, while $\eta_n(t)$ are the harmonic modal coordinates equal to $\eta_n(t) = \sin(\omega_n t + \gamma)$. The obtained solution is then:

$$\frac{EI_z}{\omega_n^2 \rho A} \frac{d^4 \phi_n(x)}{dx^4} = -\phi_n(x) \tag{3}$$

Here ω_n denotes the eigenfrequency for the n-th uncoupled vibration mode. Defining the eigenvalues β_n as

$$\beta_n = \sqrt{\omega_n} \cdot \sqrt[4]{\frac{\rho A}{EI_z}} \tag{4}$$

the assumed solution of equation (3) will be:

$$\phi_n(x) = A\sin(\beta_n x) + B\cos(\beta_n x) + C\sinh(\beta_n x) + D\cosh(\beta_n x) \tag{5}$$

Considering the relevant boundary conditions and introducing in the conventional modal model the tip mass M_t and its rotary inertia I_t, a transcendental equation is hence derived:[28-30]

$$\begin{aligned} &\left(1 + \frac{(\beta_n L)^4 M_t I_t}{m^2 L^4}\right) + \left(1 - \frac{(\beta_n L)^4 M_t I_t}{m^2 L^4}\right)(\cos\beta_n L \cosh\beta_n L) + \\ &+ \left(\beta_n L \frac{M_t}{mL} - \frac{(\beta_n L)^3 I_t}{mL^3}\right)\cos\beta_n L \sinh\beta_n L - \left(\beta_n L \frac{M_t}{mL} + \frac{(\beta_n L)^3 I_t}{mL^3}\right)\sin\beta_n L \cosh\beta_n L = 0 \end{aligned} \tag{6}$$

This equation has to be solved numerically to obtain the coefficients $\beta_n L$ and thus, via Eq. (4), the uncoupled eigenfrequencies of the cantilever ω_n.

2.2 Bending stiffness of the harvesters

To obtain the eigenfrequencies of the commercial MIDE vibration energy harvesters, their equivalent bending stiffness, expressed in terms of the EI_z product, has to be determined first. For this purpose a campaign of repetitive measurements on a VEB Thüringer Industriewerk Rauenstein tensile machine has been set-up (Fig. 3). Tests are performed on the V21b and V25w MIDE vibration energy harvesters[23] simply supported on a suitable holder. Load F is applied via a loading system mounted on the tensile machine. The applied load is measured by using a Z6FD1 HBM load cell, while deflections u of the harvester are concurrently measured by using a HBM inductive displacement transducer of the type W1T3.[31] In the considered limited range of displacements, the measured load vs. deflection data show a linear behavior, while the repeatability of the measurements is within ±2%.

Plate theory, i.e. the expression which correlates the modulus of elasticity E of a simply supported plate to its dimensions (thickness h and width b) as well as to the deflection u for a given centered point load F, where k_w is a geometrical coefficient which depends on the L/b ratio,[32] is thus used to obtain the value of Young's modulus:

$$E = \frac{12Fb^2}{k_w h^3 u} \tag{7}$$

The obtained values of the equivalent modulus of elasticity of the scavengers are then 30 GPa for the V25w and 40 GPa for the V21b scavenger type. The difference in the values is due to the different thicknesses of the layers that make up the device and the difference in the other relevant dimensions. These values can be multiplied by the overall second moment of inertia of the cross section, i.e. $I_z = (b \cdot h^3)/12$ (Fig. 4a), to obtain the equivalent bending stiffness of the considered device.

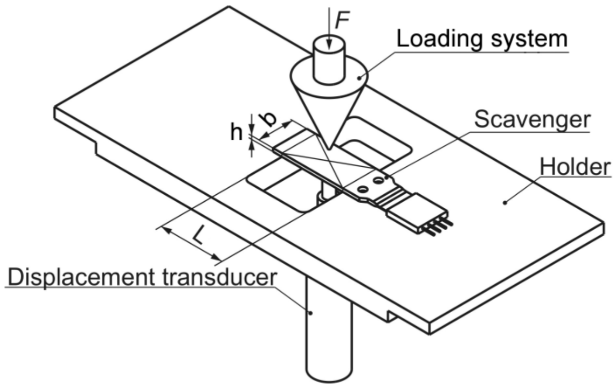

(a)

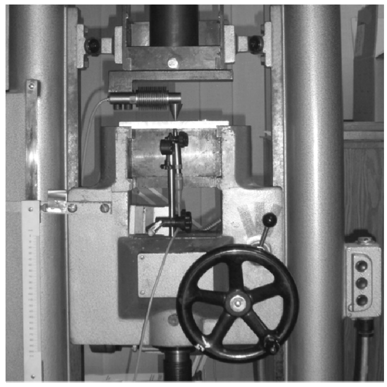

(b)

Figure 3. Experimental set-up for the determination of the equivalent bending stiffness (a) and photo of the respective lay-out (b).

An elegant yet equivalent approach to determine the equivalent bending stiffness is to use the procedure of transforming the layered cross section of the harvester (Fig. 4a) in an equivalent homogenous cross section (Fig. 4b) as defined by conventional strength of materials theory.[33] In this case the widths of the various sections are modified corresponding to the ratio of Young's modulus of that section to Young's modulus of the material chosen to be act as the reference material, while the distances of the sections from the neutral axis are kept constant. In this case copper (indicated in the figure with index "Cu") is chosen as the reference material, and thus the equivalent widths of the sections made of other materials (index "FR4" indicates the reinforced epoxy laminate sheets, index "P" the piezoelectric material, index "ES" indicates the ESPANEX laminates, while the epoxy adhesive layers are neglected) will be:

$$b_{FR4\_eq} = \frac{E_{FR4}}{E_S} b \qquad b_{P\_eq} = \frac{E_P}{E_S} b \qquad b_{ES\_eq} = \frac{E_{ES}}{E_S} b \tag{8}$$

Since the copper electrodes do not cover the whole width of the harvester, their width will in turn be:

$$b_{Cu} = 0.86b \tag{9}$$

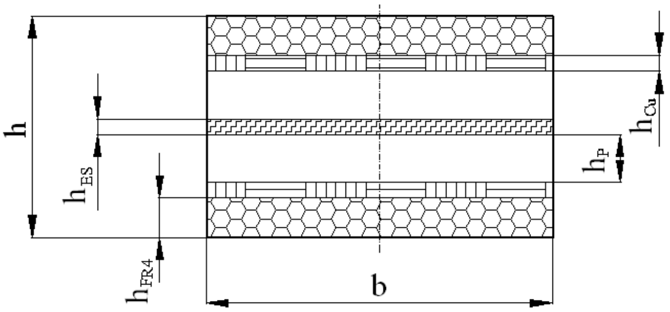

(a)

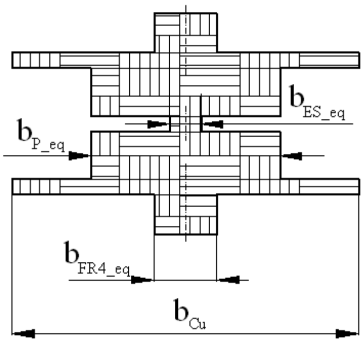

(b)

Figure 4. True (a) and equivalent (b) cross section of the multilayered vibration harvesting device.

Considering the respective layer thicknesses, and taking into consideration Steiner's rule, the equivalent second moment of inertia of the cross section of the harvester can hence be expressed as:

$$
\begin{aligned}
I_z &= 2\left(\frac{b_{FR4\_eq}h_{FR4}^3}{12}+b_{FR4\_eq}h_{FR4}\left(\frac{h_{ES}}{2}+h_P+h_{Cu}+\frac{h_{FR4}}{2}\right)^2\right)+\\
&+2\left(\frac{b_{Cu}h_{Cu}^3}{12}+b_{Cu}h_{Cu}\left(\frac{h_{ES}}{2}+h_P+\frac{h_{Cu}}{2}\right)^2\right)+2\left(\frac{b_{P\_eq}h_P^3}{12}+b_{P\_eq}h_P\left(\frac{h_{ES}}{2}+\frac{h_P}{2}\right)^2\right)+\frac{b_{ES\_eq}h_{ES}^3}{12}
\end{aligned}
\tag{10}
$$

The bending stiffnesses of the V21b and V25w type MIDE vibration energy harvesters obtained with the two methods are equivalent and equal, respectively, to the values of 0.029 and 0.008 $N \cdot m^2$.

These values are thus inserted in the uncoupled modal model developed in section 2.1. The resulting fundamental (first) uncoupled bending eigenfrequencies $\omega_n = \omega_1$ of the V21b and V25w type MIDE vibration energy harvesters are given in Table 1. In the table are reported the eigenfrequencies, expressed in the corresponding Hz values, for the harvesters loaded with 1, 2 and 3 standard MIDE tip masses (for the V21b harvester, these are the m21b MIDE standard masses, while for the V25w the standard masses are of the m20w type):[23]

Table 1. Fundamental bending eigenfrequencies of the V21b and V25w MIDE harvesters loaded with 1, 2 and 3 standard MIDE masses.

Res. freq. [Hz]	1 tip mass	2 tip masses	3 tip masses
V21b	158,8	123,9	105,1
V25w	71,2	53,1	43,8

The results in the above Table have been validated also by using the ANSYS FEM software. 2D BEAM3 and SOLID45 3D elements were hence used, while the tip mass was modeled via a MASS21 point mass element. The comparison of the results of the analytical and the FEM models allowed establishing that they always within 2% from each other, confirming thus the validity of the used uncoupled modal model.[34]

3. COUPLED DYNAMIC ANALYSYS

3.1 Experimental set-up

To validate experimentally the dynamic performances of commercially available piezoelectric vibration-based energy harvesting devices and to compare the thus obtained results with those obtained with a suitable coupled electromechanical model,[14] an experimental set-up was developed within the Laboratory for Precision Engineering of the Department of Mechanical Engineering Design of the Faculty of Engineering of the University of Rijeka.[35]

The set-up, shown in Fig. 5a, is based on a Schenk AG Vibroexciter 41 electrodynamics shaker driven via a Vibropower 41 signal generator and power amplifier. The exciter coils generate the dynamic excitation controllable in force while swept in the chosen frequency range (that can go up to 1 kHz). This harmonic excitation is transmitted to the holder and thus the scavenger. Excitation acceleration is measured via a Schenk AS-020 piezoelectric accelerometer having a 10.2 mV/(m/s^2) sensitivity and the upper measurement ranges of, respectively, 15 kHz and 800 m/s^2. The vibrations of the free end of the cantilever are measured by employing a MetroLaser VibroMet 500V 780 nm wavelength laser Doppler vibrometer with a measurement range from 5 μm/s to 800 mm/s.[36] The whole set-up in interfaced to a LabView v. 8.5 based National Instruments PXI data acquisition system.[37] The lay-out of the whole set-up is visible in Fig. 5b.

In a first instance, the dynamic response of the MIDE vibration-based energy harvesters of the type V21b and V25w is used to establish the respective mechanical damping coefficient. It was thus determined that the value of this parameter is $\zeta = 0.005$.

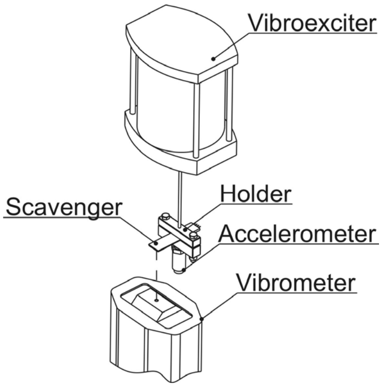

(a)

(b)

Figure 5. Experimental set-up for dynamic measurements (a) and its physical lay-out (b).

Each of the harvester devices is loaded next with the 3 mentioned MIDE standard tip masses and tested in the dynamics range around the fundamental bending resonant frequency. The downstream resistive load R_L is hence varied in a broad range of values, i.e. practically between the extremes constituted on one side by an uncoupled cantilever with R_L approaching 0 (short circuit condition) and on the other by very large R_L values (MΩ range, i.e. open circuit condition). The condition of having a pure resistive load connected to the electrodes is not necessarily the most realistic one, since often electric loads consist of rechargeable batteries and other capacitive loads. However, it is simple and useful not only for estimating the resulting power, but also for giving the designer more intuition about the system.[14, 16] What is more, a thorough study of the dynamic behavior of the harvesters in these conditions allows avoiding the problems related to the change of the sign of the strain distribution along the length of the harvester evidenced in literature,[38] increasing thus again the efficiency of energy harvesting.

The developed experimental set-up allows thus determining the FRFs of the harvesters with the piezoelectric layers electrically connected in series in terms of produced voltages – to – base acceleration and power outputs – to – base acceleration.

3.2 Coupled electromechanical model

The obtained experimental results are compared with those obtained by modeling the behavior of the used harvesters using the recently developed "coupled modal electromechanical distributed parameter model" (CMEDM) for piezoelectric vibration-based bimorphs.[14] In fact, this model is clearly more accurate in strain distribution, mode shapes and electromechanical coupling terms and is thus advantageous with respect to the previously suggested lumped parameter models.[14-15, 38] The CMEDM is based again on the Euler-Bernoulli beam assumptions, but also on the consideration of the piezoelectric backward coupling effect, i.e. on the fact that the electric field generated in the piezoelectric material (in electromechanical terms equivalent to a transformer) influences the mechanical response as well. The differential equation describing the dynamics of the harvester thus becomes:[14]

$$-\frac{\partial^2 M_z(x,t)}{\partial x^2}+c_s I_z\frac{\partial^5 u_y(x,t)}{\partial x^4 \partial t}+c_a I_z\frac{\partial u_y(x,t)}{\partial t}+m\frac{\partial^2 u_y(x,t)}{\partial t^2}=-\left[m+M_t\delta\left(x-L\right)\right]\frac{\partial^2 u_b(x,t)}{\partial t^2} \tag{11}$$

In addition to the symbols used in the previous section, here are introduced the following entities: c_s is the strain-rate damping of the material due to internal friction that is proportional to the bending stiffness of the cantilever beam,[38] c_a is the damping coefficient due to the influence of the external medium (in the considered case this is air and thus this influence is small),[38] $\delta(x)$ is the Dirac delta function (equal to 1 for $x = L$), while u_b is the effective displacement of the base of the cantilever.

Considering that bending the moment M_z depends on the stresses and strains in the layers of the piezoelectric material and performing the necessary transformations, the coupled beam equilibrium can then be expressed as:[14]

$$
\begin{aligned}
& EI_z \frac{\partial^4 u_y(x,t)}{\partial x^4} + c_s I_z \frac{\partial^5 u_y(x,t)}{\partial x^4 \partial t} + c_a \frac{\partial u_y(x,t)}{\partial t} + \\
& + m \frac{\partial^2 u_y(x,t)}{\partial t^2} + \vartheta_s v_s(t) \left[\frac{d\delta(x)}{dx} - \frac{d\delta(x-L)}{dx} \right] = -\left[m + M_t \delta(x-L) \right] \frac{\partial^2 u_b(x,t)}{\partial t^2}
\end{aligned}
\tag{12}
$$

In this equation $v_s(t)$ is the voltage across the electrodes of the serially connected piezoelectric layers, while ϑ_s is the backward coupling term defined as:[14]

$$
\vartheta_s = \frac{e_{31} b}{2h_P} \left[\frac{h_S^2}{4} - \left(h_P + \frac{h_S^2}{2} \right)^2 \right] \tag{13}
$$

where e_{31} is the effective piezoelectric stress constant, while h_S is the thickness of all non-piezoelectric layers, i.e. $h_S = h_{ES} + 2h_{FR4} + 2h_{Cu}$.

The eigenvalues β_n, i.e. the respective uncoupled eigenfrequencies ω_n are still defined by Eq. (4), while in this case the eigenfunction for the n-th mode of vibrations can be expressed as:[14]

$$
\phi_n(x) = C_n \left[\cos \beta_n x - \cosh \beta_n x + \varsigma_n \left(\sin \beta_n x - \sinh \beta_n x \right) \right] \tag{14}
$$

where

$$
\varsigma_n = \frac{\sin \beta_n L - \sinh \beta_n L + \beta_n L \dfrac{M_t}{mL} \left(\cos \beta_n L - \cosh \beta_n L \right)}{\cos \beta_n L - \cosh \beta_n L - \beta_n L \dfrac{M_t}{mL} \left(\sin \beta_n L - \sinh \beta_n L \right)} \tag{15}
$$

and the modal amplitudes C_n are obtained from the orthogonality properties of the eigenvectors. A transcendental equation identical to equation (6) describes then again the uncoupled response of the system.

For a vibration frequency ω close to the eigenfrequency ω_n and a determined downstream external resistive load R_L, the multimode FRF voltage output α_s for serially connected piezoelectric layers, related to excitation acceleration, can hence be expressed as:[14]

$$
\alpha_s(\omega) = \frac{\displaystyle\sum_{n=1}^{\infty} \frac{j\omega \kappa_n \sigma_n}{\omega_n^2 - \omega^2 + 2j\zeta\omega_n \omega}}{\dfrac{1}{R_L} + j\omega \dfrac{C_P}{2} + \displaystyle\sum_{n=1}^{\infty} \frac{j\omega \kappa_n \chi_n}{\omega_n^2 - \omega^2 + 2j\zeta\omega_n \omega}} \tag{16}
$$

In Eq. (16) j is the imaginary unit, ζ is the measured mechanical damping coefficient, while the values of the forward coupling term κ_n, the parameter σ_n, the internal capacitance of each piezoelectric layer C_P and the modal electromechanical coupling term χ_n are defined by the expressions

$$
\kappa_n = -e_{31} h_{PC} b \left. \frac{d\phi_n(x)}{dx} \right|_{x=L} \qquad \sigma_n = -m \int_0^L \phi_n(x) dx - M_t \phi_n(L) \qquad C_P = \frac{\varepsilon_{33}^S bL}{h_P} \qquad \chi_n = \vartheta_s \left. \frac{d\phi_n(x)}{dx} \right|_{x=L} \tag{17}
$$

where h_{PC} is the distance between the neutral axis and the middle of the layer of the piezoelectric material, while ε_{33}^S is the permittivity of the piezoelectric material at constant strain with the plane-stress assumption.

The herein considered single mode response at the fundamental bending eigenfrequency will obviously be obtained from equation (16) for $n = 1$. Finally, the average FRF power output of the harvester will be given by:

$$
P_{av} = \frac{\left| \alpha_s \right|^2}{2R_L} \tag{18}
$$

4. RESULTS AND DISCUSSION

The results shown in this section are those obtained for the V21b harvester loaded with two standard M21b MIDE tip masses, but they are qualitatively equivalent to those obtained for other scavenger – tip mass combinations. Quantitatively, the V25w device, loaded with comparable tip masses, yields more power than the V21b harvester since it has larger piezoelectric material volumes. The obtained power levels on the V25w harvesters are thus about twice as large as those obtained on the V21b devices, while the output powers are proportional to the tip masses.[34]

4.1 Voltage FRFs

The obtained FRFs in terms of the achieved steady state voltages – to – harmonic base acceleration for varying resistive loads R_L, where the excitation frequencies are expressed in terms of their ratio to the uncoupled configuration of the harvester, are shown in Fig. 6 and allow establishing that:

- There is a good match between the experimental and the results obtained by employing the CMEDM (Fig. 6a).
- The observed differences are probably due to effects that are not included in the CMEDM, i.e.:
  - the influence of the adhesive layers neglected in the model,
  - the eventual non-perfect bonding of the layers in the harvester device,
  - the combined influence on the mechanical response of the system given by:
    - the anticlastic effect, which was recently shown to have a significant nonlinear hardening effect on the dynamic behavior of vibrating cantilevers that, in turn, depends on the amplitude of the excitation as well as on the position on the beam and on the dynamics of each oscillation cycle,[39]
    - the large (geometrically nonlinear) deflections,[40]
    - the compliance of the fixture which can be hardly estimated and controlled,
    - the parametric uncertainties due to measurement errors and to the variability of the characteristic parameters during manufacturing and operation treated recently in literature.[11]
- There is an appreciable influence of the voltage feedback due to the piezoelectric effect on the dynamic response, i.e. the coupled electromechanical response of the system under consideration is much more complex than the mere mechanical modal model could predict.
- This effect leads to an increase of the modal frequency where the value of the output voltage becomes maximal, with respect to the uncoupled modal frequency ω_n, by more than 4% (Fig. 6b).
- The increase of the external resistive load R_L causes also a marked nonlinear increase of the amplitude of the maximal output voltages (from 1.7 to more than 8 V/(m/s^2)).

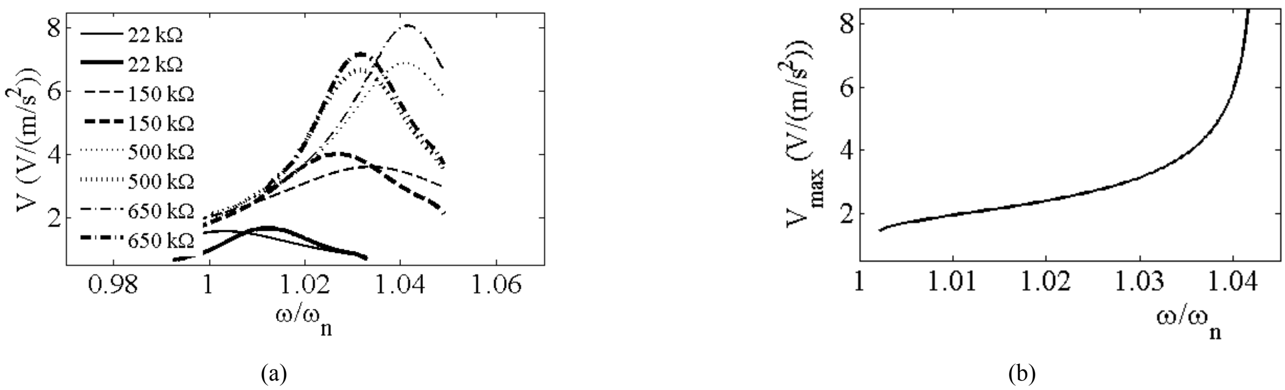

Figure 6: Voltage FRFs obtained experimentally (thick lines) and via the CMEDM (thin lines) for R_L values from 22 to 650 kΩ (a) and CMEDM maximal voltages vs. ω/ω_n for R_L values in the kΩ to MΩ range (b).

4.2 Power FRFs

The FRFs in terms of the obtained power outputs– to – harmonic base acceleration are expressed here in terms of average powers normalized to the volume of the piezoelectric material in the harvesting device. The obtained results allow establishing that:

- There is again a good match between the experimental and the analytical results (Fig. 7a – for clarity reasons only the curves obtained for two values of R_L are shown).
- The maximal reached average specific power levels in the considered case are at about 28 μW/(m/s^2)^2/mm$^3_{PZT}$.
- The maximal average power vs. resistive load dependency is complex and not monotonic (Fig. 7b). In fact, initially there is a decrease of the maximal average powers with increasing R_L with a subsequent amplification and then again a decrease for the largest applied loads. The dependency allows, however, the optimal resistive load, i.e. that which results in the largest output power, to be determined. It is interesting to note here that there can be several R_L values that, for a certain excitation frequency, can result in the same value of the maximal average specific power.

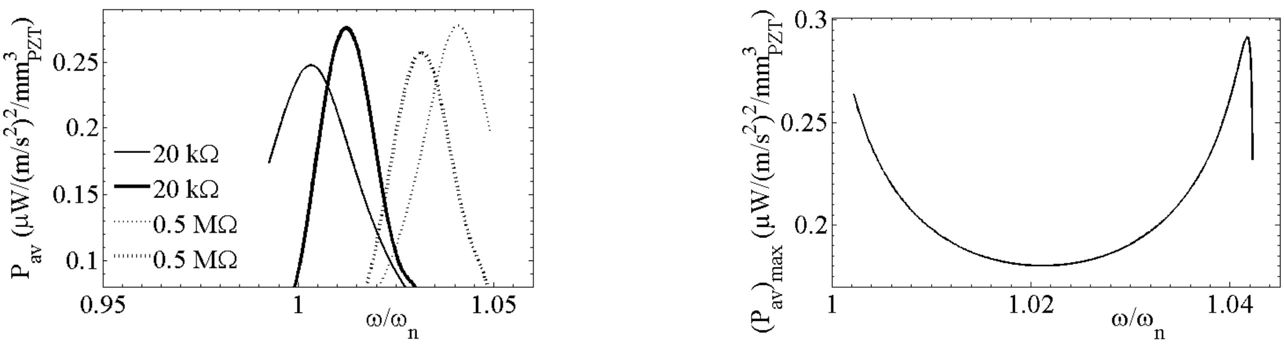

(a) (b)

Figure 7: Power FRFs obtained experimentally (thick lines) and via the CMEDM (thin lines) for R_L = 22 kΩ and R_L = 0.5 MΩ (a) and CMEDM maximal average powers vs. ω/ω_n for R_L values in the kΩ to MΩ range (b).

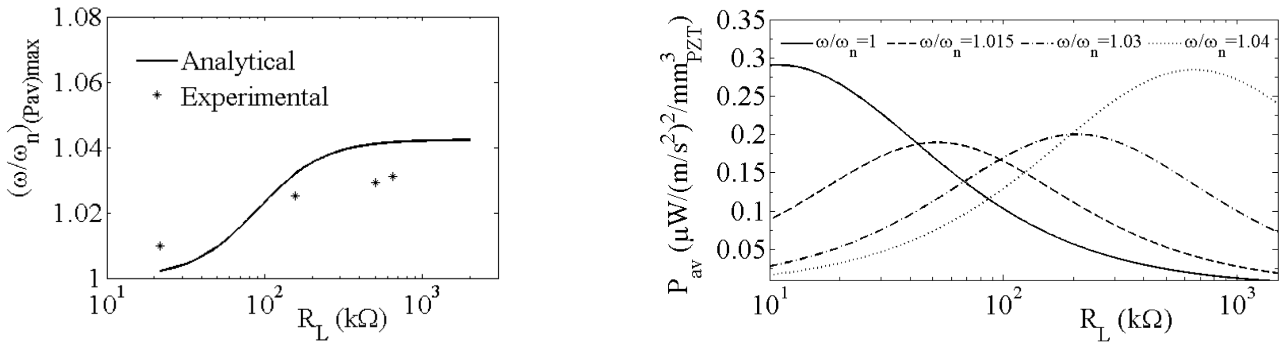

(a) (b)

Figure 8: Experimental and CMEDM ratio of frequency where the average specific power is maximal to ω_n vs. R_L (a) and variation of the CMEDM average specific power outputs vs. R_L for different excitation frequencies from short circuit to open circuit condition.

- There is a clear nonlinear hardening behavior, quantitatively slightly different experimentally than analytically, which, for increasing R_L values, augments by roughly 4% the frequencies where the maximal average powers are obtained (Fig. 8a). This hardening, which can be appreciated analytically only when the coupled electromechanical behavior is modeled via the CMEDM, in the considered case has a marked increase for loads of up to about R_L = 300 kΩ, while subsequently the amplification is much slower up to the open circuit conditions.

- There is a large variation of the optimal R_L values where the average specific output powers will be maximal for varying excitation frequencies. This is again something that can be appreciated correctly only when the coupled electromechanical behavior of the piezoelectric vibration-based harvesting devices is modeled via the CMEDM (Fig. 8b).
- The lowest electrical loads will, obviously, give a maximal average specific power output for excitation frequencies corresponding to the short circuit condition, while the highest loads will be giving maximal average specific power outputs for frequencies approaching the open circuit condition. Intermediate excitation frequencies give smaller maximal specific average powers even for optimized R_L values.

5. CONCLUSIONS

In this work a thorough experimental and analytical investigation of the performances of commercially available piezoelectric vibration energy harvesters is performed. Their eigenfrequencies are determined first by employing the uncoupled modal model where the equivalent bending stiffness of the complex cross section of the harvesters is determined either experimentally or by employing conventional strength of materials theory. The study of the dynamic behavior allows then establishing the dependence of the voltage and power outputs on harmonic excitation and electrical loads, as well as determining the loads and frequencies where the maximal voltage and power levels are obtained. While an increase of the loads has a clear hardening effect on the dynamic behavior of the considered devices, the maximal obtainable powers have a complex dependence on the loads. The dependence of the power on the loads and excitation frequencies can be used to match the power to the actual needs of a specific application. All these effects can be appreciated analytically only by using the recently proposed coupled modal electromechanical distributed parameter model.

The obtained results will be used in the next phase of the work in the design of a new class of piezoelectric vibration-based energy harvesting devices that will be optimized for a set of design criteria which may include not only their electromechanical dynamic behavior but also dimensional constraints and material strength limits.

ACKNOWLEDGEMENTS

The performed work is supported by the "Ultra-high precision compliant devices for micro and nanotechnology applications" project of the Croatian Ministry of Science, Education and Sports.

The authors thank for their kind help the Laboratory of Mechanics of the University of Udine, the Metallurgical Laboratory Friuli Innovazione of Udine, the Laboratory for Strength Analysis and the Laboratory for Machine Dynamics of the Faculty of Engineering of the University of Rijeka.

REFERENCES

[1] Priya, Sh. and Inman, D. J. (ed.), [Energy Harvesting Technologies], Springer, New York, (2009).
[2] De Marqui, C. J., Erturk, A. and Inman, D. J., "An electromechanical finite element model for piezoelectric energy harvester plates," J. Sound Vibr. 327, 9-25 (2009).
[3] Paradiso, J. A. and Starner, Th., "Energy Scavenging for Mobile and Wireless Electronics," IEEE Perv. Comp., 18-27 (2005).
[4] Roundy, S. et al., "Improving Power Output for Vibration-Based Energy Scavengers," IEEE Perv. Comp., 28-36 (2005).
[5] Starner, Th. and Paradiso, J. A., "Human Generated Power for Mobile Electronics," in C. Piguet (ed.), [Low-Power Electronics], CRC Press, Boca Raton, Chapter 45 (2004).
[6] www.greennpower.com

[7] www.energyharvestingjournal.com
[8] www.holstcentre.com
[9] www.jennic.com
[10] Roundy, S., "On the Effectiveness of Vibration-based Energy Harvesting," J. Int. Mat. Sys. Struct. 16, 809-823 (2005).
[11] Ali, S. F., Friswell, M. I. and Adhikari, S., "Piezoelectric energy harvesting with parametric uncertainty," Smart Mater. & Struct. 19, 105010 (2010).
[12] Anton, S. R. and Sodano, H. A., "A review of power harvesting using piezoelectric materials (2003-2006)," Smart Mater. & Struct. 16/3, R1 (2007).
[13] Beeby, S. P., Tudor, M. J. and White, N. M., "Energy harvesting vibration sources for microsystems applications," Meas. Sci. Technol. 17, R175–R195 (2006).
[14] Erturk, A. and Inman, D. J., "An experimentally validated bimorph cantilever model for piezoelectric energy harvesting from base excitation," Smart Mater. & Struct. 18(2), 025009 (2009).
[15] Erturk, A. and Inman, D. J., "Issues in mathematical modelling of piezoelectric energy harvesters," Smart Mater. & Struct. 17, 065016 (2008).
[16] Roundy, S. and Wright, P. K., "A piezoelectric vibration based generator for wireless electronics," Smart Mat. & Struct. 13, 1131-1142 (2004).
[17] Roundy, S., Wright, P.K. and Rabaey, J., "A study of low level vibrations as a power source for wireless sensor nodes," Comp. Comm. 26, 1131–1144 (2003).
[18] Sodano, A., Inman, D. J. and Park, G., "Comparison of Piezoelectric Energy Harvesting Devices for Recharging Batteries," J. Int. Mat. Sys. Struct. 16, 799-807 (2005).
[19] www.advancedcerametrics.com
[20] www.adaptivenergy.com
[21] www.arveni.fr/eng_home.php
[22] www.enocean.com/en/home
[23] www.mide.com/products/volture/volture_catalog.php
[24] www.perpetuum.com
[25] www.olympusamerica.com/seg_section/product.asp? product=1017&p=57&sub=2
[26] www.x-raymicroanalysis.com/x-ray-microanalysis-explained/pages/main/main.htm
[27] Genta, G., [Vibration of structures and machines - III ed.], Springer, New York, (1998).
[28] Bailey, Th. L., [Distributed-parameter vibration control of a cantilever beam using a distributed-parameter actuator – M. Sc. thesis], Massachusetts Institute of Technology, Boston, 116-119 (1984).
[29] Clough, R. Y. and Penzien, J., [Dynamics of structures – 3rd ed.], Computers & Structures, Berkeley, 377-384 (2003).
[30] Meirowitch, L., [Fundamentals of Vibrations], McGraw Hill, Boston, (2001).
[31] www.hbm.com
[32] Stiglat, K. and Wippel, H., [Platten], W. Ernst, Berlin, (1973).
[33] Timoshenko, S. and MacCullough, G. H., [Elements of Strength of Materials – 2nd ed.], Van Nostrand, New York, (1944).
[34] Blazevic, D. and Zelenika, S., "Characterisation of vibration energy harvesters," Proc 20th Int. DAAAM Sym., 1837-1838 (2009).
[35] www.riteh.hr/zav_katd_sluz/zvd_kons_stroj/katedre/konstruiranje/laboratoriji/nano_lab/Prec_Lab_aktivnost.htm
[36] www.metrolaserinc.com
[37] www.ni.com
[38] Erturk, A. and Inman, D. J., "On Mechanical Modelling of Cantilevered Piezoelectric Vibration Energy Harvesters," J. Intel. Mat. Sys. Struct. 19, 1311-1325 (2008).
[39] De Bona, F., Zelenika, S. and Munteanu, M. Gh., "Mechanical properties of microcantilevers: Influence of the anticlastic effect," Sens. Act. A 165(2), 431-438 (2011).
[40] De Bona, F. and Zelenika, S., "A generalized Elastica-type approach to the analysis of large displacements of spring-strips," J. Mech. Eng. Sci. – Proc. Inst. Mech. Eng. C 211, 509-517 (1997).